Progress In Electromagnetics Research Letters, Vol. 102, 47–55, 2022

High Performance CPW Fed Printed Antenna with Double Layered Frequency Selective Surface Reflector for Bandwidth and Gain Improvement

Harikrishna Paik[1, *], Shailendra K. Mishra[1], Chadalvada M. Sai Kumar[1], and Khambam Premchand[2]

Abstract—An aperture coupled printed antenna using frequency selective surface (FSS) reflector is reported in this paper. The proposed antenna includes two layers of FSS reflectors designed with an array of 7×5 crossed elements on the top substrate to achieve wideband, high gain, and improved directivity. The antenna implements an aperture coupled radiating element on the bottom substrate which serves as the source feed antenna to the FSS reflector. The proposed structure has an overall dimension of $30 \times 32 \times 1.6\,\text{mm}^3$ operating between 6.5 and 8.3 GHz with an impedance bandwidth of 1.8 GHz. The results reveal that the impedance bandwidths in excess of 82.3% and 44.5% have been achieved compared to the source feed antenna and antenna with single layer FSS, respectively. Further, the peak gain of 6.25 dB has also been achieved in the operational frequency band with a two-layer FSS which is 29.4% and 15.8% more than the antenna without FSS and antenna with single FSS layer. Due to compact structure, wideband, high gain, and fabrication simplicity, the proposed antenna may be suitable for long distance communication systems.

1. INTRODUCTION

Ultra-wideband (UWB) systems have been widely used in applications including wireless short range communications, sensors, and imaging systems. The high potential of these systems for short pulse transmission and handling large data transmission rates has led to more focused research in this field [1]. Further, authorization by the Federal Communication Commission for the use of unlicensed spectrum from 3.1 to 10.6 GHz has increased the demand for the design of printed antenna. Several printed configurations of slot and monopole antennas have been demonstrated for the use in UWB systems [2, 3]. These antennas provide excellent impedance bandwidth at lower frequency, but suffer from poor radiation characteristics and directivity in the upper band of operation, typically beyond 6 GHz. Further, the omnidirectional behaviour is not optimal for the short distance line of sight application which requires a limited angular range, since most of the power is radiated in the unwanted directions [4]. Hence, in order to provide a good impedance bandwidth with high antenna gain and directivity a printed antenna with a double layered FSS has been proposed. Therefore, the idea of designing a high performance printed antenna in terms of bandwidth and radiation characteristics without altering its original structural design has always been of interest to researchers in the field of Electromagnetics. Surveying the literature reveals that several antennas have been reported to achieve these characteristics with significant renewed interest in the recent years. These include antenna with electromagnetic bandgap structures [5], magnetic monopole and dipole antennas [6], metamaterial based

Received 17 October 2021, Accepted 16 December 2021, Scheduled 5 January 2022

* Corresponding author: Harikrishna Paik (pavan_paik2003@yahoo.co.in).

[1] Department of Electronics and Communication Engineering, Veltech University, Chennai, India. [2] Department of Electronics and Communication Engineering, VRSEC, Vijayawada, India.

antennas [7], spiral antenna [8], and resonant cavity antennas [9]. Since these antennas operate in the fundamental dipole mode as their physical sizes are small relative to the operational wavelength, it is difficult to achieve high gain and high directivity, especially when there is a relatively small or no ground plane in the antenna.

Several techniques have been employed to achieve high performance of the antenna. Moreover, with the introduction of frequency selective surface (FSS) structures in the recent years, antennas with different sizes and shapes have been designed to achieve broadband characteristics with high gain and high directivity [10, 11]. It has been shown that by loading the conventional antenna with FSS periodic structures, high performance in terms of gain, wideband, and directivity are attainable [12]. These antennas are based on metamaterial negative refractive index transmission-line theory in which the source is loaded with capacitors and inductors to achieve desired resonance. This unique property has led to the design of antennas with improved directivity, gain, and radiation characteristics employing FSS structures. Besides, the miniaturization capabilities of the antennas can also be engineered [13].

Several reports on FSS based antenna to achieve broadband characteristics, high gain, and high directivity have been published [14–18]. In [14], a dual band monopole antenna using two FSS layers consisting of 5×6 elements corner reflectors placed at 90° is reported. The antenna is designed to resonate at 3 GHz and 5.5 GHz. Using this structure, an improved impedance bandwidth of 24% and antenna gain of 8–10 dBi have been realized. Besides, the distance between the antenna and perpendicularly placed FSS layers results in measurement errors. A coplanar waveguide fed UWB monopole antenna (61 mm $\times$ 61 mm $\times$ 1.6 mm) with single layer FSS using 10×10 array unit cells is presented in [15]. This structure showed an impedance bandwidth of 8.85 GHz covering the UWB range from 3.05 to 11.9 GHz. In addition, an improvement in the gain of 6.22 dB from 1.65 dB to 7.87 dB in the whole frequency band has also been realized. Nevertheless, the implementation of six cylinders to construct strawberry shaped radiating element increases the complexity in the design.

Attia et al. [16] presented a wideband and high-gain Fabry-Perot cavity printed antenna (14.8 mm $\times$ 18 mm $\times$ 2.5 mm) operating at 60 GHz. This structure composed of two partially reflective FSS layers (4×4 element array) to achieve wideband characteristics and high 3 dB gain bandwidth. Results show that the maximum gain of 16.8 dB has been realized, and the 3 dB gain bandwidth of 12.5% from 58.6 to 66.4 GHz has also been achieved in the whole operating bandwidth. In spite of these, the implementation of metallic vias and printed ridge gap waveguide feed structure makes the structure bulky. In [17], a wideband circularly polarized planar dipole antenna ($123 \times 123 \times 0.8\,\text{mm}^3$) using an FSS superstrate for reducing radar cross section is designed. The FSS layer is implemented using an array of 5×5 square loop elements. Using this structure, the impedance bandwidth of 2.15 GHz in the frequency band of 0.95–3.1 GHz and 3-dB axial ratio bandwidth of 0.45 GHz over 1.9–2.35 GHz have been achieved. Further, the reduction in average radar cross section of 6.9 dB has also been realized with 5.9 dB improvement in antenna gain in the whole operational frequency band. Besides, the antenna application is restricted due to low bandwidth. In addition, the FSS reflector is placed at a large gap from the antenna which may result in measurement error in the experimentation. In [18], a patch antenna combined with an artificial magnetic conductor (AMC) ground plane and an FSS superstrate is presented. The antenna results in a 3-dB axial ratio bandwidth of 20% in the whole operating bandwidth and a gain up to 16 dBi. However, the array of diagonal rectangular slots used in the AMC ground plane increases the design complexity and makes the structure bulky.

In this paper, a coplanar waveguide fed, low profile printed antenna with two FSS layers is reported. First, an aperture coupled printed antenna with a rectangular patch is designed on the bottom substrate which serves as a radiating source to the FSS reflector. Then, two layers of FSS structures consisting of 7×5 crossed elements are designed on the top substrate separated by an air gap. The FSS layers serve as a partially reflective surface which improves the directivity and gain of the antenna. The whole structure is designed on FR4 substrates with permittivity of 4.4, loss of tangent 0.02, and thickness of 1.6 mm. The structure is simulated using HFSS simulator, and performances of the antenna are analyzed. A prototype of the structure is fabricated, and measured results are validated with simulation results.

2. ANTENNA GEOMETRY AND DESIGN

The structure of the proposed antenna is shown in Figure 1(a). As shown in the figure, the antenna consists of an inverted L shaped cavity resonator in the ground plane and a rectangular radiating patch at the top surface of the bottom substrate which serves as the feeding source. The source antenna is excited using coplanar waveguide feed which resonates at 6.6 GHz. Two layers of FSS reflectors consisting of 7×5 crossed elements are designed on the lower and upper surfaces of the top substrate to achieve wide bandwidth and high gain. The unit cell of the FSS reflector is implemented using the crossed element, whose length and width determine the resonant frequency. For optimum performance, the two substrates are separated by an air gap at a distance equal to thickness of the substrate. The whole structure is designed using a pair of FR4 substrates, each of thickness 1.6 mm, permittivity 4.4, and loss tangent 0.02.

Figure 1(b) shows the cavity resonator with the patch and cross sectional view of the feed antenna and FSS reflector. As depicted in Figure 1(b), W_F and L_F are the width and length of the feed line. W_1 is the gap between the coplanar waveguide feed line and ground plane. W_2 and L_2 denote the aperture

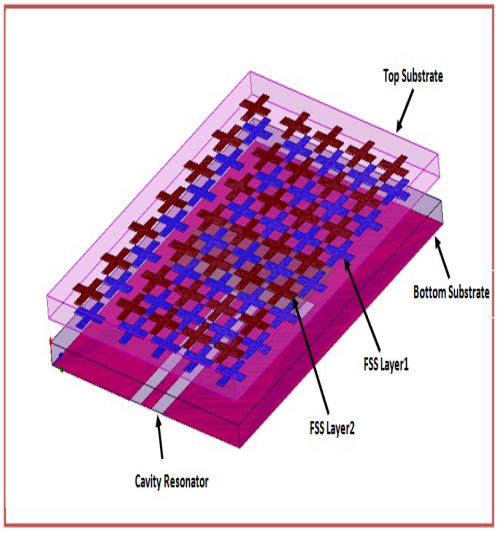

(a)

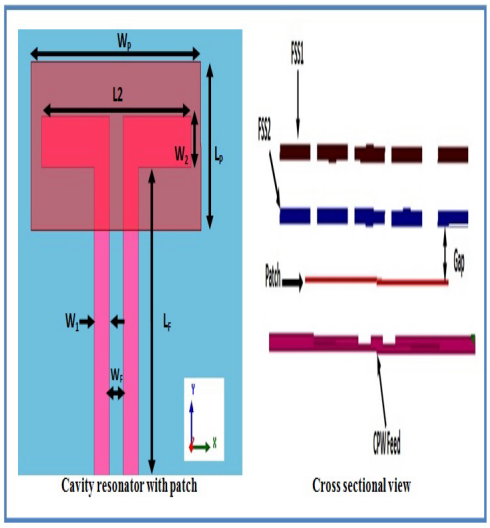

(b)

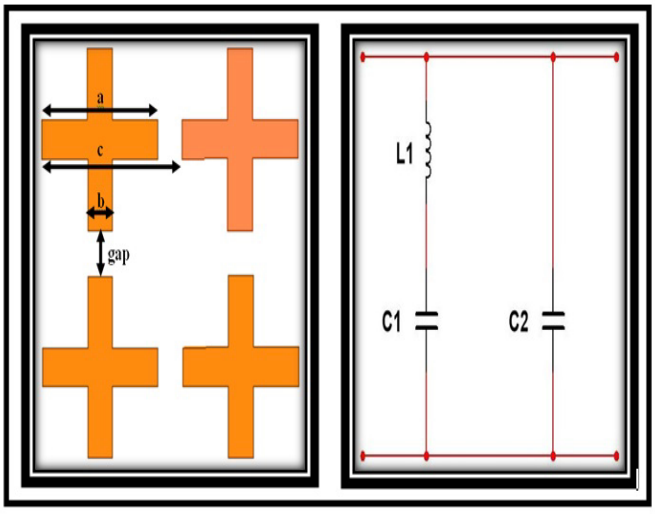

(c)

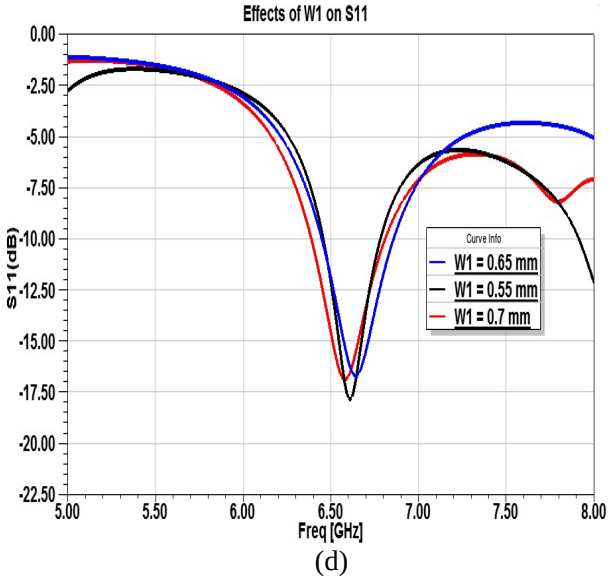

(d)

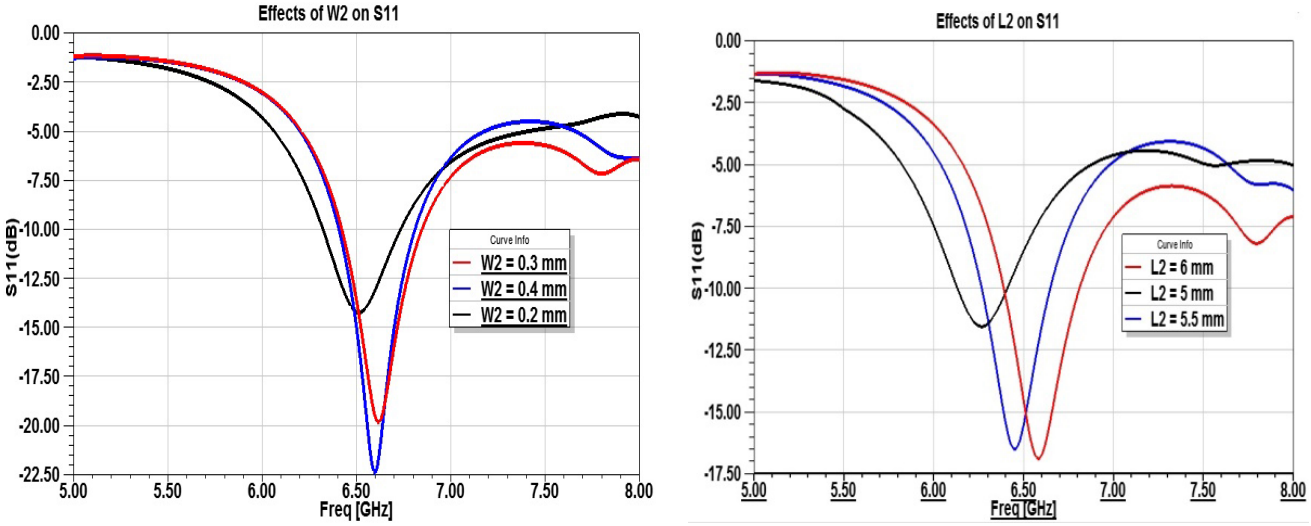

Figure 1. (a) Antenna structure, (b) cavity resonator and cross sectional view, (c) unit cell crossed element and equivalent circuit model, (d) S_{11} for different values of W_1, (e) effects of W_2 on S_{11}, (f) effects of L_2 on S_{11}.

width and length, and L_P and W_P represent the length and width of the rectangular radiating element. Primarily, the antenna dimensions are determined based on analytical equations of the aperture, patch, and feed. Then, the antenna parameters are optimized using HFSS software.

Figure 1(c) shows the geometry of the crossed element implanted in the FSS layer and its equivalent circuit. It is seen from the equivalent circuit that the vertical crossed elements are modeled as transmission line conductors, and the gap between these two elements is modeled as series loading capacitors. The horizontal arms of the crossed elements are modeled as a shunt capacitor. As can be seen from Figure 1(c), L_1 is the inductance of the dipole of length (a) and width (b). C_1 represents the capacitance between the vertical dipoles gap, and C_2 is the capacitance between the horizontal dipoles. The unit cell crossed element resonates at a frequency (f_0), when the length of the unit cell is equal to $\lambda_0/2$, where λ_0 is the free space wavelength. Therefore, the FSS structure can be viewed as a tuned network with LC elements. The resonant frequency is determined by adjusting the values of L_1 and C_1. The detailed dimensions of a unit cell cross element are: length (a) = 4.5 mm, width (b) = 1 mm, and c = 5.5 mm (periodicity). The length of the unit cell and resonant frequency (f_0) are determined by following equations:

$$a = \frac{c_0}{4f_0\sqrt{(\varepsilon_r + 1)}} \tag{1}$$

$$f_0 = \frac{1}{2\pi\sqrt{L_1 C_1}} \tag{2}$$

where C_0 is the free space velocity; ε_r denotes the relative permittivity; f_0 is the resonant frequency; L_1 and C_1 correspond to inductance and capacitance of the dipole.

The proposed antenna is designed for operation over 6.5–8.3 GHz covering C and lower X band frequency. To obtain optimum performance of the antenna, parametric study is carried out. The simulation results for different values of feed line width (W_1) are shown in Figure 1(d). It can be seen that the operational bandwidth is reduced at lower values of W_1, typically for $W_1 = 0.55$ and 0.65 mm due to impedance mismatch between the feed line and the source antenna. Therefore, $W_1 = 0.7$ mm is selected to be the optimum value. The width (W_2) and length (L_2) of the cavity resonator are varied, and their effects on S_{11} are plotted as shown in Figure 1(e) and Figure 1(f), respectively. The results reveal that with increasing the resonator width and length, the quality of reflection coefficient and impedance bandwidth are notably improved. At the same time, the resonant frequency is shifted to higher frequencies.

The optimized dimensions of the antenna obtained from parametric study are given in Table 1.

Table 1. Proposed antenna dimensions.

parameter	Size (mm)	parameter	Size (mm)
W_1	0.7	L_2	6
W_F	1.2	W_2	0.3
L_F	20	a	4.5
W_P	16	b	1
L_P	8	c	5.5

3. RESULTS AND ANALYSIS

3.1. Return Loss, S_{11}

The simulation results of return loss, S_{11} of the aperture coupled antenna without FSS, with single and double layer FSS are depicted in Figure 2(a). It can be seen that the source feed antenna without FSS layer operates from 6.5 to 6.8 GHz with an impedance bandwidth of 300 MHz. It is noted that the antenna bandwidth spans over 1 GHz from 6.8 to 7.8 GHz with single FSS layer. A significant improvement in bandwidth is achieved which extends from 6.5 to 8.3 GHz with two layers of FSS. Thus, the antenna with two layers FSS shows broadband performance with an excess bandwidths of 82.3% and 44.5% compared to the source feed antenna without FSS and antenna with single FSS layer. However, the improvement in bandwidth of the whole antenna structure is due to the FSS structures which serve as the reflector.

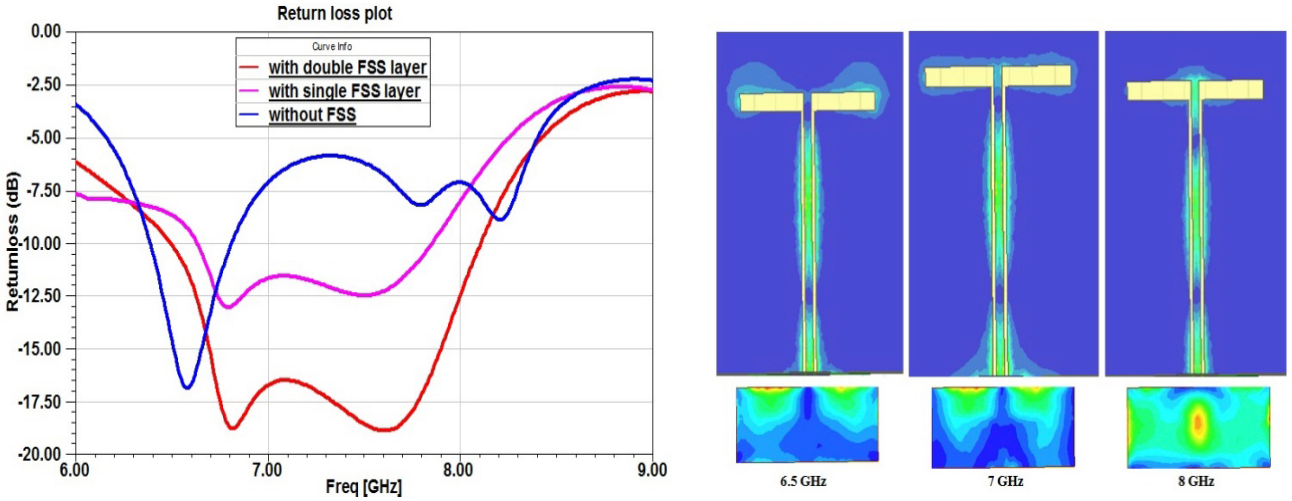

(a) (b)

Figure 2. (a) Return loss without and with FSS, (b) surface current distribution at 6.5, 7 and 8 GHz.

To further investigate the performance of the proposed antenna, the surface current distributions at typical operational frequencies are depicted in Figure 2(b). It is observed that the surface current at lower frequencies is concentrated at the top edge of the resonator and upper edge of the patch. Thus, reducing the gain at the lower frequencies. It can be pointed out that, at higher frequency, the current is distributed uniformly through the patch surface with a more saturated current at the center.

3.2. Antenna Gain and Radiation Efficiency

The simulation results of antenna gain and radiation efficiency of the source feed antenna, for antenna with single and double FSS layers are shown in Figure 3. It is observed from Figure 3(a) that the antenna without FSS achieves the peak gain of 4.25 dB at a typical frequency of 7.5 GHz, where it is 4.75 dB and 5.5 dB for the antenna with single and double FSS layers, respectively. This establishes that the antenna with double FSS layers improved the gain by 29.4% and 15.8% in comparison with the source feed antenna and antenna with single FSS layer. It should be noted that the proposed antenna presents a composite design in terms of directivity and radiation characteristics, and hence the gain of the antenna does not increase with frequency.

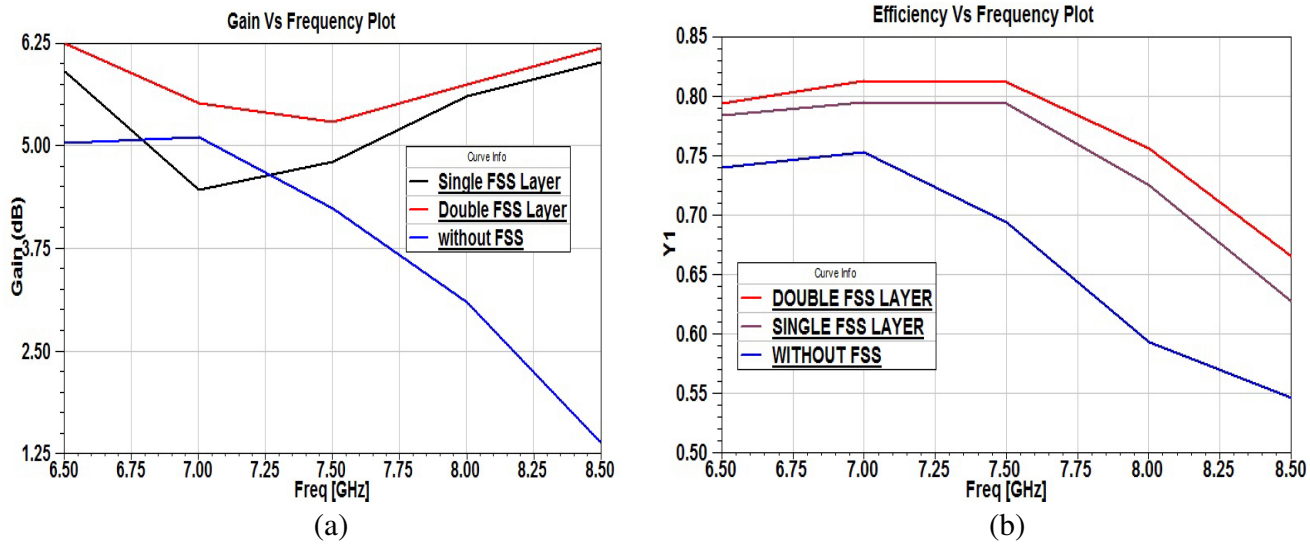

Figure 3. (a) Simulated gain, (b) radiation efficiency.

Further, the radiation efficiencies of three different antenna structures are depicted in Figure 3(b). It is seen that the antenna with double FSS layers has a radiation efficiency of 81% while it is 79% and 75% for antenna with single FSS layer and antenna without FSS, respectively. Thus, it can be established that the introduction of double FSS layers enhanced the radiation efficiency of the antenna.

4. MEASUREMENT AND EXPERIMENTAL RESULTS

Figure 4 shows a prototype of the fabricated antenna. Initially, a cavity resonator is etched at the ground plane of the lower substrate, and a rectangular patch is designed at the top surface of the substrate. Then, FSS layers designed at either sides of the top substrate are added to complete the structure. The measurements are performed using Agilent N5230 vector Network analyzer, and a 50 Ω cable is used as the antenna port.

The simulated and measured S parameters are depicted in Figure 5(a). It is revealed that the bandwidth of the antenna for the return loss less than −10 dB is about 24.32% (6.5–8.3 GHz), covering the frequency band required for long distance radio communication. There is an acceptable agreement between simulation and measurement results. However, the experienced deviations are attributed to the measurement errors. Figure 5(b) shows the comparisons between the measured and simulated gains of the antenna. It is established that the maximum gain of 6.25 dB is realized in the operational frequency band. A good agreement is observed between the simulated and measured results. The small deviations might be due to the misalignment between the antenna layers.

To demonstrate the performance of the antenna, the simulated and measured co-polarization (solid) and cross-polarization (dashed) plots at typical frequencies of 7 and 8 GHz are depicted in Figure 6. A

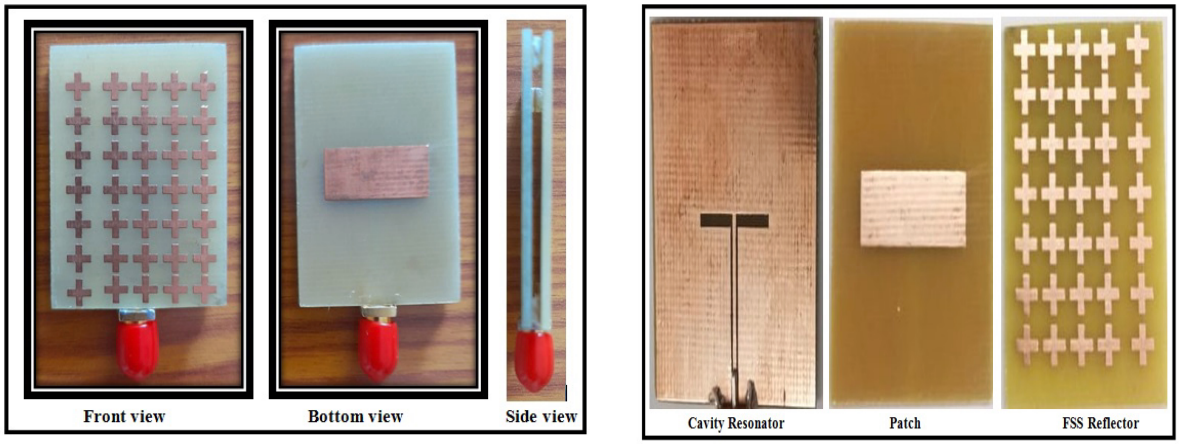

(a) (b)

Figure 4. A prototype of the proposed antenna: Front view, bottom view and side view.

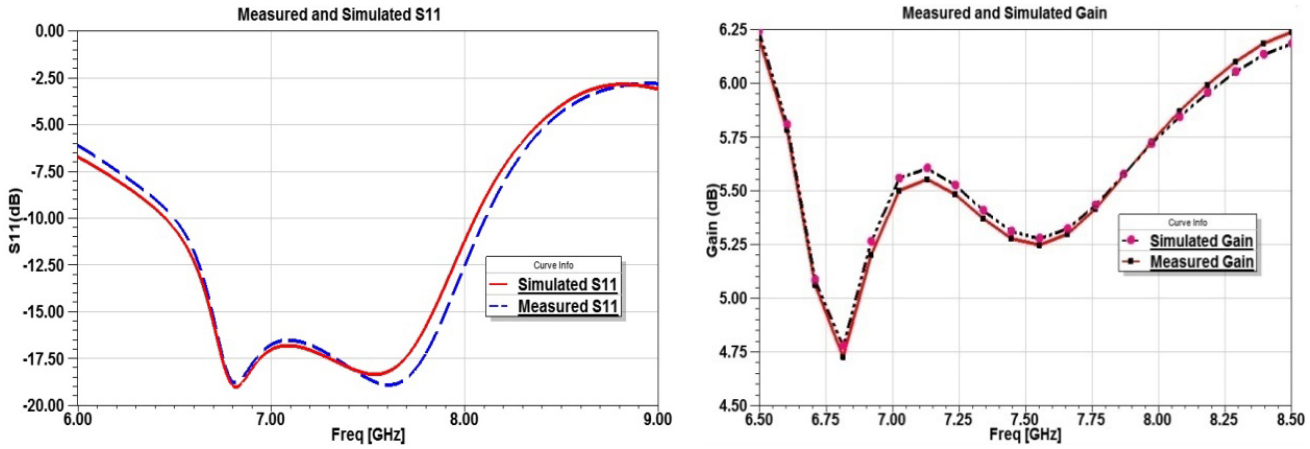

(a) (b)

Figure 5. (a) Measured and simulated S-parameter, (b) measured and simulated antenna gain.

good agreement is observed between the simulated and measured results, especially around the broadside direction. The cross-polarization levels of the simulated and measured results are well below -22 dB.

A comparison of performance of the proposed antenna with those reported in the literature is given in Table 2.

A careful observation indicates that the proposed design has small dimension and implements

Table 2. Comparison of performance.

Ref.	Antenna Size (mm^3)	Size & No of FSS layer	Frequency (GHz)	Bandwidth (%)	Gain (dB)	Efficiency (%)
[14]	$110 \times 110 \times 1.6$	10 mm × 8 mm & 2	3 & 5.5	24	8–10	–
[15]	$61 \times 61 \times 1.6$	6 mm × 6 mm & 1	3.05–11.9	118	7.87	94
[16]	$59 \times 72 \times 2.53$	14.8 mm × 18 mm & 1	55.4–66.6	18.4	15.6	–
proposed	$30 \times 32 \times 1.6$	4.5 mm × 4.5 mm & 2	6.5–8.3	24.32	6.25	81

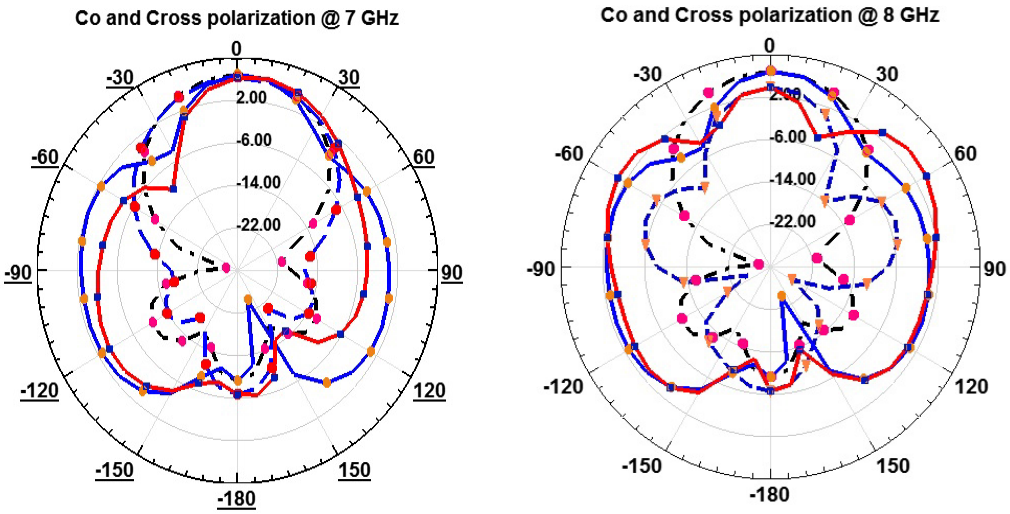

Figure 6. (a) Measured and simulated copolarization and cross polarization at 7 and 8 GHz.

small size unit cell as compared to the antenna in [14–16]. It is noted that the bandwidth of the present structure is more than that of the antenna in [16] and comparable with the design in [14], but less than that in [15]. Further, the peak gain enhancement of the proposed design is comparable with the antenna in [14] and [15]. The design methods used in [15] and [16] are based on a single layer planar FSS structure, whereas the proposed scheme applies two layers planar FSS reflectors.

5. CONCLUSION

A printed antenna using cavity resonator with two layers of FSS structures has been designed. It is established that the antenna with two layers of FSS reflectors contributes significant improvement in bandwidth with an average of 63% in comparison to source feed antenna and antenna with single layer FSS. It is shown that the antenna with double FSS layers exhibits improvement in the gain by 29.4% and 15.8% in comparison with the source feed antenna and antenna with single FSS layer, respectively. It is established that the presented design is small in size and implements small size unit cell elements as compared to the structures reported in the literature. The appreciable bandwidth and gain of the proposed design may be suitable for long distance communication systems.

REFERENCES

1. Immoreev, I. Y., "Practical applications of UWB technology," *IEEE Aerospace and Electronic Systems Magazine*, Vol. 25, No. 2, 36–42, 2010.
2. Nasimuddin, X. Qing, and Z. N. Chen, "A wideband circularly polarized stacked slotted microstrip patch antenna," *IEEE Antennas and Propagation Magazine*, Vol. 55, No. 6, 84–99, 2013.
3. Kang, D., G. Cheng, Y. Wu, D. Qu, and Z. Bing, "A broadband circularly polarized printed monopole antenna with parasitic ," *IEEE Antennas and Wireless Propagation Letters*, Vol. 16, 2509–2512, 2017.
4. Nicolas, F., D. Jean-Yves, K. Georges, and S. Robert, "Design optimization of UWB printed antenna for omnidirectional pulse radiation," *IEEE Transactions on Antennas and Propagation*, Vol. 56, No. 7, 1875–1881, 2008.
5. Chen, D., W. Yang, and W. Che, "High-gain patch antenna based on cylindrically projected EBG planes," *IEEE Antennas and Wireless Propagation Letters*, Vol. 17, No. 12, 2374–2378, 2018.

6. Liang, Z., Y. Li, X. Feng, J. Liu, and Y. Long, "Microstrip magnetic monopole and dipole antennas with high directivity and a horizontally polarized omnidirectional pattern," *IEEE Transactions on Antennas and Propagation*, Vol. 66, No. 3, 1143–1152, 2018.
7. Bai, C. X., Y. Z. Cheng, Y. R. Ding, and J. F. Zhang, "A metamaterial-based S/X-band shared-aperture phased-array antenna with wide beam scanning coverage," *IEEE Transactions on Antennas and Propagation*, Vol. 68, No. 6, 4283–4292, 2020.
8. Luo, Q., S. Gao, M. Sobhy, J. Li, G. Wei, and J. Xu, "A broadband printed monofilar square spiral antenna: A circularly polarized low-profile antenna," *IEEE Antennas and Propagation Magazine*, Vol. 59, No. 2, 79–87, 2017.
9. Hashmi, R. M. and K. P. Esselle, "A class of extremely wideband resonant cavity antennas with large directivity-bandwidth products," *IEEE Transactions on Antennas and Propagation*, Vol. 64, No. 2, 830–835, 2016.
10. Akbari, M., S. Gupta, M. Farahani, A. R. Sebak, and T. A. Denidni, "Gain enhancement of circularly polarized dielectric resonator antenna based on FSS superstrate for MMW applications," *IEEE Transactions on Antennas and Propagation*, Vol. 64, No. 12, 5542–5546, 2016.
11. Rabia, Y., N. Akira, I. Makoto, and T. A. Denidni, "A novel UWB FSS-based polarization diversity antenna," *IEEE Antennas and Wireless Propagation Letters*, Vol. 16, 2525–2528, 2017.
12. Narayanan, S., G. Gulati, B. Sangeetha, and U. N. Ravindranath, "Novel metamaterial-element-based FSS for airborne radome applications," *IEEE Transactions on Antennas and Propagation*, Vol. 66, No. 9, 4695–4704, 2018.
13. Wei, P.-S., C.-N. Chiu, C.-C. Chou, and T.-L. Wu, "Miniaturized dual-band FSS suitable for curved surface application," *IEEE Antennas and Wireless Propagation Letters*, Vol. 19, No. 12, 2265–2269, 2020.
14. Chatterjee, A. and S. K. Parui, "Performance enhancement of a dual-band monopole antenna by using a frequency-selective surface-based corner reflector," *IEEE Transactions on Antennas and Propagation*, Vol. 64, No. 6, 2165–2171, 2016.
15. Al-Gburi, A. J. A., I. Ibrahim, M. Y. Zeain, and Z. Zakaria, "Compact size and high gain of CPW-fed UWB strawberry artistic shaped printed monopole antennas using FSS single layer reflector," *IEEE Access*, Vol. 8, 2697–2707, 2020.
16. Attia, H., M. Lamine Abdelghani, and T. A. Denidni, "Wideband and high-gain millimeter-wave antenna based on FSS Fabry-Perot cavity," *IEEE Transactions on Antennas and Propagation*, Vol. 65, No. 10, 5589–5594, 2017.
17. Sharma, A., B. K. Kanaujia, S. Dwari, D. Gangwar, S. Kumar, H. C. Choi, and K. W. Kim, "Wideband high-gain circularly-polarized low RCS dipole antenna with a frequency selective surface," *IEEE Access*, Vol. 7, 6592–6602, 2019.
18. Rasoul, F. and A. Iman, "Compact Fabry-Perot antenna with wide 3-dB axial ratio bandwidth based on FSS and AMC structures," *IEEE Antennas and Wireless Propagation Letters*, Vol. 19, No. 8, 1326–1330, 2020.